JOURNAL OF BACTERIOLOGY, Apr. 1997, p. 2373–2381 Vol. 179, No. 7
0021-9193/97/$04.00+0

Generation of Buds, Swellings, and Branches instead of Filaments after Blocking the Cell Cycle of *Rhizobium meliloti*

JUDITH N. LATCH AND WILLIAM MARGOLIN*

Department of Microbiology and Molecular Genetics, University of Texas Medical School, Houston, Texas 77030

Received 9 October 1996/Accepted 30 January 1997

Inhibition of cell division in rod-shaped bacteria such as *Escherichia coli* and *Bacillus subtilis* results in elongation into long filaments many times the length of dividing cells. As a first step in characterizing the *Rhizobium meliloti* cell division machinery, we tested whether *R. meliloti* cells could also form long filaments after cell division was blocked. Unexpectedly, DNA-damaging agents, such as mitomycin C and nalidixic acid, caused only limited elongation. Instead, mitomycin C in particular induced a significant proportion of the cells to branch at the poles. Moreover, methods used to inhibit septation, such as FtsZ overproduction and cephalexin treatment, induced growing cells to swell, bud, or branch while increasing in mass, whereas filamentation was not observed. Overproduction of *E. coli* FtsZ in *R. meliloti* resulted in the same branched morphology, as did overproduction of *R. meliloti* FtsZ in *Agrobacterium tumefaciens*. These results suggest that in these normally rod-shaped species and perhaps others, branching and swelling are default pathways for increasing mass when cell division is blocked.

Rod-shaped bacteria such as *Escherichia coli* grow by elongation and segregate their chromosomes to either side of the future division site (8). When cell division is blocked either directly, as in *fts* mutants, or indirectly, by treatment with DNA-damaging agents or in strains with mutations affecting DNA synthesis or segregation, cells continue to increase in mass by elongating into filaments many times the length of dividing cells (3). Filamentation in these cases is thought to be due to inhibition of the septation initiator FtsZ or other Fts proteins involved in subsequent steps of cell division (2). A nondividing *E. coli* cell with intact, segregated chromosomes can be considered a concatemer of unit-length cells which, if division is resumed, can give rise to many cells. Thus, the filamentation process is a way to preserve the architectural and genomic integrity of bipolar unit cells in the predivisional state. Under certain conditions, this maintenance of the bipolar rod shape in bacteria which are normally rod-shaped can be perturbed. Some *E. coli* cells containing the *ftsL* mutation form short branches (13). In addition, a small proportion of *E. coli* cells containing mutations affecting chromosome replication or segregation also can form buds or branches in minimal medium (1). These branches retain the shape characteristics of the mother cell, in particular the diameter. However, it seems clear that at least for *E. coli*, as well as for many other bacteria, including *Bacillus subtilis*, the default pathway for growth during cell division inhibition is elongation, not branching.

Rhizobium meliloti exists both as a free-living form in the soil and as a nitrogen-fixing bacteroid in leguminous plants (17). Several lines of evidence indicate that its cell division cycle may be different from that of *E. coli*. First, *R. meliloti* contains two novel *ftsZ* genes with divergent C termini; the smaller of the two, *ftsZ2*, appears to be nonessential for free-living growth (20). Second, *R. meliloti* contains three stable chromosome-like elements (25) which must be replicated and segregated before each cell division, implicating a more stringent control over DNA dynamics than that of *E. coli*. Third, whereas most free-living forms are rod shaped, most bacteroids are Y shaped, indicating that a morphological transition occurs during the differentiation process. Since bacteroids are nondividing, one possibility is that blocking the cell cycle in *R. meliloti* leads to branching. Large proportions of branched cells have been documented for free-living rhizobia grown in certain specialized media (15, 28). In addition, a mutant of *Agrobacterium tumefaciens*, another member of the *Rhizobiaciae*, forms Y-shaped cells at the nonpermissive temperature (10). Since filamentous morphology in free-living *Rhizobium* bacteroids had not been reported, we were interested in determining whether filaments could ever be generated in free-living *R. meliloti* after blocking the cell division cycle. Here we use several approaches which all suggest that the way *R. meliloti* normally deals with cell division inhibition while still increasing cell mass is by creation of new growth sites. We also suggest that this mechanism is conserved in *Agrobacterium* species.

MATERIALS AND METHODS

Bacterial strains, plasmids, and chemicals. *E. coli* LE392 was used for tests with drugs, and strains JM109, DH5α, and XL1-Blue were used to harbor plasmids. *R. meliloti* WM249 and MB501 are derivatives of Rm1021 (21) with transposon insertions permitting the efficient electroporation of *E. coli* plasmid DNA; WM249 contains a Tn*5-233* element encoding gentamicin resistance (20), whereas MB501 (obtained from M. Barnett, Stanford University) contains the same Tn*5-233* swapped for trimethoprim resistance. *A. tumefaciens* A136 is strain C58 cured of the Ti plasmid (31). Plasmids pWM176, pWM186, and pWM189 are tetracycline-resistant, broad-host-range plasmids containing P_{tac}, P_{tac}-*ftsZ2*, and P_{tac}-*ftsZ1*, respectively (20). Plasmid pMK3 is pWM176 with *E. coli ftsZ* oriented opposite P_{tac}, and pMK4 is the same except that the *E. coli ftsZ* insert is inverted, allowing expression to be driven by P_{tac}.

Cephalexin, nalidixic acid, and mitomycin C were all from Sigma Chemical Company. Stock solutions of cephalexin and mitomycin C were prepared at concentrations of 1 and 0.5 mg/ml, respectively, in H_2O and stored at −20°C in small aliquots. A nalidixic acid stock solution was prepared at a concentration of 2.5 mg/ml in 0.01 N NaOH, pH 9, and stored at 4°C.

Growth conditions. For drug treatments, *R. meliloti* strains were grown at 28°C in TY (0.6% tryptone, 0.3% NaCl, 0.05% $CaCl_2$) broth or agar supplemented with 500 μg of streptomycin per ml and 10 μg of tetracycline per ml for plasmid maintenance. For FtsZ overproduction, *R. meliloti* was grown in LB (per liter, 10 g of tryptone, 5 g of yeast extract, and 5 g of NaCl) supplemented with streptomycin and tetracycline, and *A. tumefaciens* was grown in TY plus tetracycline; both species were grown at 28 to 30°C. LE392 was grown in LB at 37°C.

Induction conditions. For time course induction experiments, *R. meliloti* MB501 or *E. coli* LE392 was grown to early logarithmic phase (optical density at 600 nm [OD_{600}], 0.1), diluted twofold, and then regrown to an OD_{600} of 0.1.

* Corresponding author. Mailing address: Department of Microbiology and Molecular Genetics, University of Texas Medical School, Houston, TX 77030. Phone: (713) 500-5452. Fax: (713) 500-5499. E-mail: margolin@utmmg.med.uth.tmc.edu.

Nalidixic acid (12 μg/ml), mitomycin C (200 ng/ml), or isopropyl-β-D-thiogalactopyranoside (IPTG; 1 mM) was then added. For *R. meliloti*, at time zero and every 2 h thereafter, OD_{600} measurements were taken with a Shimadzu UV160U spectrophotometer and cell counts were determined with a 20-μm-deep Petroff-Hausser bacteria counter (C. A. Hausser & Son, Philadelphia, Pa.). Each small square (50 by 50 μm) has a volume of 5×10^{-8} ml. The average number of cells per square from 20 squares was determined and was multiplied by 2×10^7 to obtain the number of cells per milliliter. Graphs were created by using the SigmaPlot software from Jandel Scientific (San Rafael, Calif.). MICs were determined by plating approximately 100 bacteria per plate on media containing various concentrations of drugs and noting the minimum concentration of drug that resulted in no colonies.

For FtsZ protein overproduction and light microscopy, a stock solution of 400 mM IPTG in *N*,*N*-dimethylformamide was added to cells at an OD_{600} of 0.1 to a final concentration of 1 mM. In the time course experiment, cells were then monitored for growth and cell number as described above and photographed at intervals. Otherwise, cells were induced with IPTG in mid-logarithmic phase and grown for 12 h before microscopic observation. The same procedure was used for preparing cells for electron microscopy (EM) except that cells were at an OD_{600} of 0.5 when induced with IPTG and were grown 10 to 12 additional hours.

Microscopic techniques. For EM, 1 ml of cells was fixed in a solution consisting of 2% glutaraldehyde and 1% paraformaldehyde in 0.1 M phosphate buffer (pH 7.0), washed, treated with 1% OsO_4, washed in phosphate buffer, stained with 2% uranyl acetate, washed again, and then dehydrated in an ethanol series. All manipulations were done in microcentrifuge tubes, with spins at $14{,}000 \times g$ at room temperature. For transmission EM (TEM), samples were embedded in Spurr's medium (27), sectioned to 60- to 90-nm widths, stained with lead citrate, and viewed with a Philips 410 transmission electron microscope. Samples for scanning EM (SEM) were resuspended in a 50:50 mixture of 100% ethanol and 100% hexamethyldisilazane and then in 100% hexamethyldisilazane; 20 μl of the sample was transferred to stubs, dried, and coated to a thickness of 12 nm with a Polaron high-resolution gold sputter coater. The samples were viewed with a Philips 505 scanning electron microscope.

To isolate bacteroids for SEM, alfalfa (Iroquois) was grown in agar medium in tubes and inoculated with Rm1021 as described previously (22). After 6 weeks, several mature, pink nodules were harvested and then crushed with a plastic homogenizer in 0.5 ml of 10 mM $MgSO_4$, and the total mixture was prepared for EM as described for the 1 ml of cells above except that 3% glutaraldehyde and 2% paraformaldehyde were used.

Cells for light microscopy were either placed directly between a glass slide and a coverslip or first immobilized by mixing a 50:50 mixture of cells and molten 2% agarose or low-melting-point agarose in LB medium. Cells were viewed with a Zeiss Axioskop or an Olympus BX60 microscope under a 40× (for cell counting) or a 100× oil immersion objective with either differential interference contrast or phase-contrast optics. Images were obtained either by photography with Kodachrome Elite 400 film or by acquisition with an Optronics DEI-750 video camera followed by digitization. Digital images were manipulated in Adobe Photoshop 3.0 and printed on a Tektronix Phaser 440 dye sublimation printer.

RESULTS

Effects of DNA-damaging agents on *R. meliloti* growth and morphology. *E. coli* normally forms filaments when its DNA replication is inhibited, due to direct effects on chromosome segregation and indirect effects on cell division via the SOS response (6, 14). To interfere with DNA replication of *R. meliloti*, we treated *R. meliloti* MB501 with nalidixic acid and mitomycin C. In *E. coli*, nalidixic acid inhibits gyrase function, ultimately causing double-stranded breaks in the DNA which can be repaired by RecBCD (24). Mitomycin C directly causes double-stranded breaks in DNA. Both drugs induce the SOS response in *E. coli* (6, 14). We found that for *R. meliloti* MB501, the MIC of nalidixic acid was 2 to 4 μg/ml and that of mitomycin C was less than 50 ng/ml. This compared with nalidixic acid and mitomycin C MICs for *E. coli* LE392 of 2 to 4 μg/ml and about 200 ng/ml, respectively.

Exponentially growing LE392 and MB501 cultures were exposed to nalidixic acid, and its effects on growth and morphology are shown in Fig. 1. Whereas the drug caused the *E. coli* cells to elongate many times the length of untreated cells after growth for several hours (Fig. 1C, compare top and middle panels at left), the *R. meliloti* cells elongated only two- to threefold even after 10 h of growth (Fig. 1C, right panels). A partial explanation for this is that nalidixic acid treatment moderately inhibited cell mass increase, allowing only a 5.2-fold total mass increase compared to a 7.5-fold increase for the untreated control between 2 and 10 h after drug addition (Fig. 1A). However, during this time span, cell numbers increased by only 1.6-fold in cultures with nalidixic acid, compared with a 9.3-fold increase for the control. The calculated mass increase per cell was 3.3-fold for nalidixic acid and 0.8-fold for the control. These data are consistent with the observed cell length increases and suggest that both cell mass increase and cell division were inhibited by the drug. Although nalidixic acid is specific for DNA synthesis in many bacteria, it has been shown to block RNA synthesis as well as DNA synthesis in *Caulobacter crescentus* (7). It is likely that this type of nonspecific action by nalidixic acid was responsible for the inhibition of *R. meliloti* growth accompanying the inhibition of cell division. Polar branches became visible in some cells at the 10-h time point (Fig. 1C) and were also seen with much greater frequency during mitomycin C treatment (see below). These branches are consistent with an effect on cell division since branching is a likely way for a cell to increase mass when its division is blocked.

The effects of mitomycin C were more specific and dramatic than those of nalidixic acid. Once again, although *E. coli* formed long filaments many times the length of normally dividing cells (Fig. 1C, compare top and bottom panels at left), the average end-to-end length of *R. meliloti* cells increased only two- to threefold (Fig. 1C, right panels). As with nalidixic acid, the increase in cell mass also correlated with the appearance of polar branches, resulting in Y-shaped cells. However, branched cells were observed much sooner after drug addition (less than 6 h), and the proportion of branched cells was at least 50% at 10 h, much higher than that observed with nalidixic acid. The proportion of cells containing branches as well as the lengths of the branches increased with time over the course of the experiment. Some cells at 10 h even exhibited branching at both poles (Fig. 1C). As with nalidixic acid, the effects on cell mass and number were measured. As expected, the amount of cell mass increase relative to the increase in cell numbers was higher with mitomycin C: over the 2- to 10-h time span, mass increased 6.1-fold (Fig. 1A) while cell number increased only 1.3-fold (Fig. 1B). The calculated mass increase per cell for this time span was 4.7-fold, which is consistent with the length increase plus the additional mass increase due to the branching. These data support the idea that mitomycin C is more specific than nalidixic acid at blocking *R. meliloti* cell division, presumably via the DNA replication cycle. For both drugs, most of the cell number increase occurred in the first 2 h (Fig. 1B), before the drugs exerted their full effect. The increases were probably due to division of cells that had completed DNA replication and segregation prior to drug addition.

Although *E. coli* nucleoids become aggregated or degraded in the presence of mitomycin C or nalidixic acid, staining of cells with 4′,6-diamidino-2-phenylindole (DAPI) revealed that only a small number of *R. meliloti* cells treated with either of these drugs had a distinct aggregated nucleoid (data not shown). It is not clear why most cells appeared to be full of DNA. Perhaps this could be explained by the slightly larger genome size and smaller cell size of *R. meliloti* versus *E. coli*, as well as the potentially complex topology due to the tripartite nature of the *R. meliloti* chromosome (25).

Effects of cephalexin on *R. meliloti* cell morphology. Cephalexin is an inhibitor of penicillin binding protein 3 (PBP3, also known as FtsI), which functions specifically in the synthesis of septum peptidoglycan (26). Therefore, in *E. coli*, blocking PBP3 either with cephalexin or by mutation results in continued elongation into filamentous cells with indentations at the blocked division sites. *R. meliloti* was very sensitive to cepha-

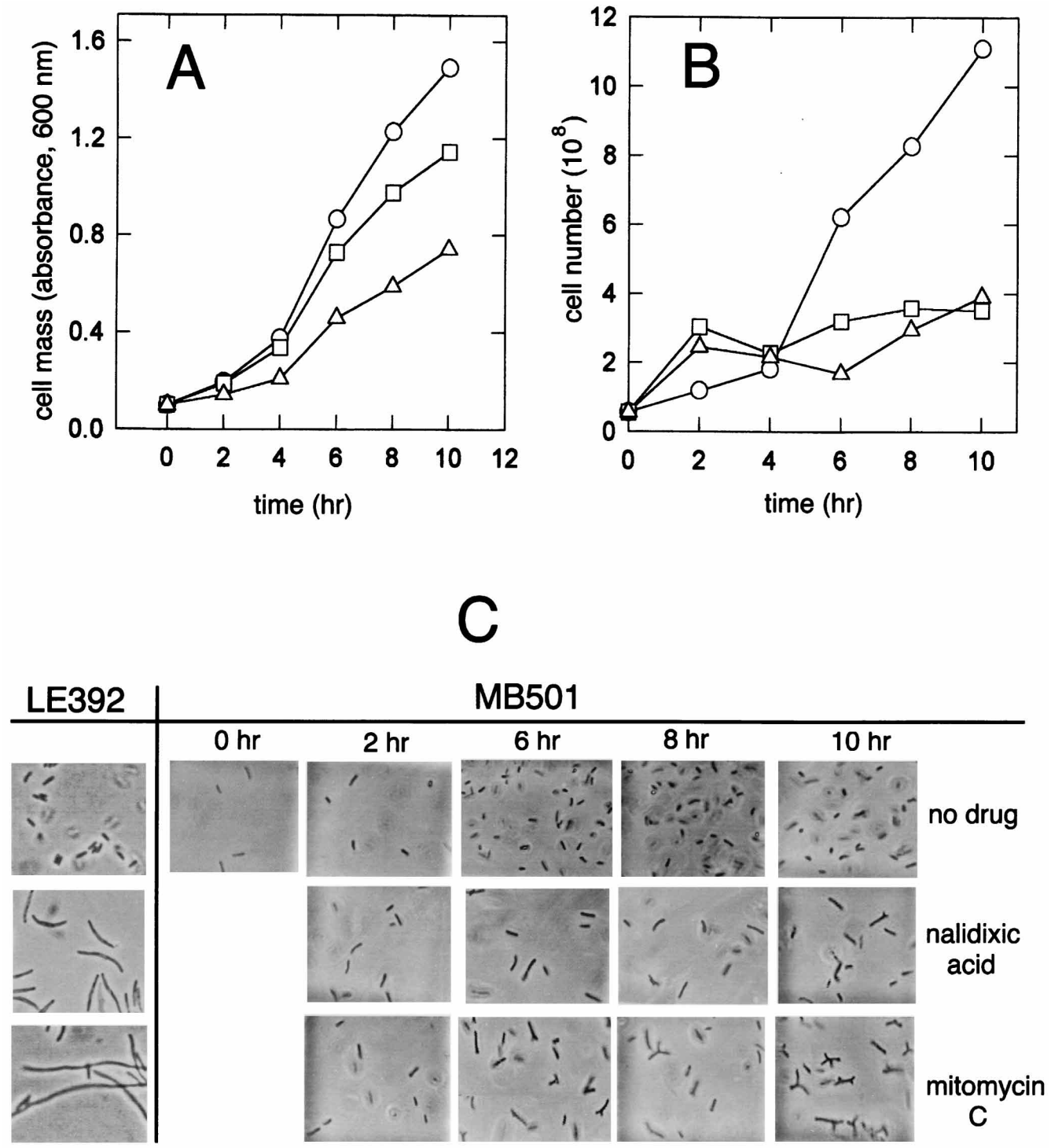

FIG. 1. Effects of mitomycin C and nalidixic acid on cell growth, division, and morphology. All data shown are from a single time course experiment. (A and B) *R. meliloti* MB501 was grown as described in Materials and Methods and was treated with either no drug (circles), 12 μg of nalidixic acid per ml (triangles), or 200 ng of mitomycin C per ml (squares) at time zero and sampled every 2 h for determination of the OD_{600} (A) and cell number (B). (C) The same samples were examined by phase-contrast microscopy; a representative field is shown for each time point. For comparison, *E. coli* LE392 cells are shown after treatment for several hours with no drug, 12.5 μg of nalidixic acid per ml, or 200 ng of mitomycin C per ml. Bar = 10 μm.

lexin; the MIC of this drug for *R. meliloti* was 0.2 μg/ml, while it was 2 to 4 μg/ml for *E. coli*. Cephalexin-induced filaments of *E. coli* are shown in Fig. 2D. Treatment of *R. meliloti* MB501 with cephalexin above the MIC caused a significant proportion of cells to bud or lyse at midcell. Interestingly, some of these cells also contained multiple branches (Fig. 2B and data not shown). High cephalexin levels caused the lysis to become more severe until the cells became protoplasts (data not

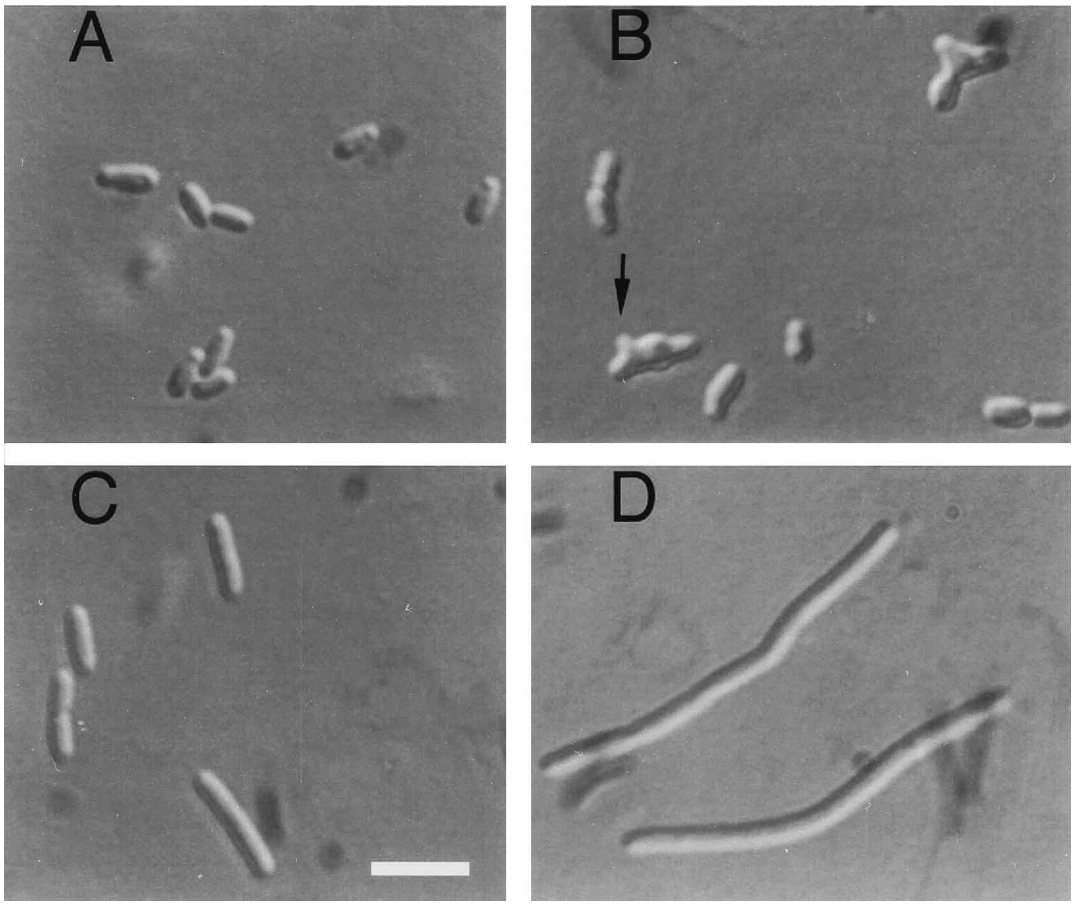

FIG. 2. Effects of cephalexin on cell morphology. (A) *R. meliloti* MB501; (B) MB501 with 3 μg of cephalexin per ml, showing branches and swellings (arrow); (C) *E. coli* LE392; (D) LE392 with 3 μg of cephalexin per ml. Drug was added to exponentially growing cells, which then were allowed to grow for several additional hours. Images were taken with differential interference contrast optics. Bar = 4 μm.

shown). Levels of cephalexin at or below the MIC caused a small proportion of MB501 cells to swell at midcell, but none exhibited significant elongation (data not shown). There are two likely explanations for these results. First, even at low concentrations, cephalexin may have nonspecific effects in *R. meliloti* and may target PBPs other than PBP3, resulting in lysis at the growing septum region first and, eventually, lysis of the whole cell before elongation can occur. Second, there may be more than one PBP involved in septation in *R. meliloti*, or perhaps PBP3 has a different role in *R. meliloti* than in *E. coli*. However, the significant proportion of cells containing multiple branches along with midcell swellings suggests the possibility of a cell division block occurring simultaneously with cell wall lysis. Furthermore, the presence of branched cells and absence of filamentous cells with various levels of cephalexin is consistent with our hypothesis that *R. meliloti* cells branch but do not form filaments.

Overproduction of either *R. meliloti* FtsZ protein causes branching and swelling of *R. meliloti* cells. When *E. coli* FtsZ levels are severalfold higher than those of wild-type *E. coli*, minicells are produced due to stimulation of polar septation events in excess of the midcell events. When FtsZ levels are increased further, septation is completely inhibited, resulting in cell filamentation (30). This inhibition may be due to aberrant localization or structure of the FtsZ polymers (18). In view of the unusual response of *R. meliloti* to perturbations of its cell cycle and its possession of two unique *ftsZ* genes, we wanted to test directly the hypothesis that blocking septation in *R. meliloti* would not result in filamentation. Despite the fact that *ftsZ2* is nonessential and no conditional mutant of *ftsZ1* exists, the effects of FtsZ overproduction in *E. coli* suggested that overproduction of either *ftsZ* in *R. meliloti* might cause a cell division defect that could mimic such a mutant.

The two *R. meliloti ftsZ* homologs, *ftsZ1* and *ftsZ2*, are present on broad-host-range plasmids pWM189 and pWM186, respectively, under the control of $lacI^q$ and the *tac* promoter. IPTG induction of *R. meliloti* WM249 cells containing these plasmids results in protein overproduction detectable by Coomassie staining (20). IPTG induction of *E. coli* strains containing pWM189 (P_{tac}-*ftsZ1*) causes cell filamentation, similar to the effects by a P_{lac}-*ftsZ1* derivative described previously (19), whereas induction of pWM186 (P_{tac}-*ftsZ2*) appears to cause filamentation mainly on solid media (20).

To overproduce FtsZ proteins in *R. meliloti* for cell division inhibition studies, we induced WM249 cells carrying pWM186 or pWM189 with IPTG in early logarithmic phase and measured their density, numbers, and morphology over time. Whereas cell mass increased five- to sixfold between 0 and 9 h postinduction, cell numbers only doubled for pWM189 and decreased slightly for pWM186 cells (data not shown). Cells were examined by light microscopy at several time intervals (Fig. 3) and, in a different experiment, by SEM (Fig. 4). As with the DNA replication inhibition experiments, we found no filamentous cells. Instead, overproduction of FtsZ1 after IPTG

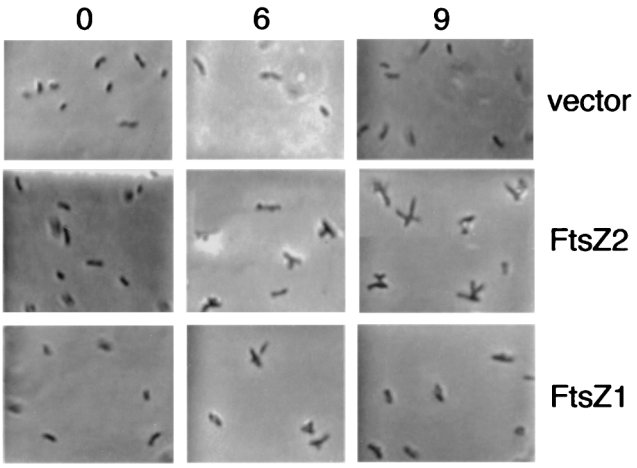

FIG. 3. Time course of *R. meliloti* cells overproducing FtsZ1 and FtsZ2. Phase-contrast images of WM249/pWM176 (vector), WM249/pWM186 (FtsZ2), and WM249/pWM189 (FtsZ1) cells are shown at various times (in hours) after IPTG induction. Bar = 5 μm.

induction caused many cells to increase their mass by swelling at their midpoints and by producing branches. The midcell swellings became noticeable at 4 to 6 h postinduction (Fig. 3, bottom center panel). These branched cells were often T shaped (Fig. 3, bottom right panel; Fig. 4F), in contrast to the generally Y-shaped cells observed with mitomycin C (Fig. 1). Many cells exhibited multiple branches and invaginations, giving them a lumpy appearance. The branches were often located at midcell, at the presumptive division site. Cells that contained just the plasmid vector alone that were induced with IPTG were generally normal in appearance (Fig. 3, top panels; Fig. 4A), despite the occasional appearance of branched cells, analogous to the small percentage of filamentous cells in some *E. coli* cultures. Also normal in appearance were uninduced cells carrying pWM189 (Fig. 4E). Interestingly, some cells displayed double constrictions at the division site, making a central minicell (Fig. 4A); this phenomenon was also seen with FtsZ2 overproduction (Fig. 4D) and may hint at a different mechanism of septation in *R. meliloti.* cells. One dividing cell in Fig. 4A had a branch at one pole, indicating that branching and septation can occur simultaneously in the same cell.

The effects of FtsZ2 overproduction with IPTG induction were similar but more exaggerated, perhaps because of the significantly higher levels of FtsZ2 relative to FtsZ1 both before and after IPTG induction (20). Although uninduced cells with pWM189 (*ftsZ1*) were normal in appearance, uninduced pWM186 (*ftsZ2*) cells were abnormal (Fig. 4C). Upon induction with IPTG, this abnormal morphology was greatly increased, with branching and budding being observed in virtually all cells (Fig. 4B). Branches were first observed at 3 h postinduction, correlating with the first decrease in cell number, and the degree of branching increased with time as cell mass increased (Fig. 3, middle row of panels). Often cells contained multiple branches which in turn contained bulges or additional branches (Fig. 4D). Some cells displayed bulges at the division site, similar to those seen after cephalexin treatment (Fig. 4B).

To confirm that these phenotypes were due to cell division inhibition and were not a general effect of protein overproduction, we also examined *R. meliloti* cells overproducing green fluorescent protein (GFP). These cells produced large amounts of protein, as visualized by green fluorescence and by Coomassie blue staining of protein by sodium dodecyl sulfate-polyacrylamide gel electrophoresis. The staining of gels showed that at least as much GFP was produced as FtsZ after IPTG induction. Nevertheless, the GFP-overproducing cells were all rod shaped (data not shown). This suggests that the morphological features of branching and swelling are specific to a cell division block and are not a nonspecific effect due to protein overproduction.

Other aspects of the physiology of the *R. meliloti* FtsZ overproducers also were consistent with cell division defects. For example, the number of viable cells of *R. meliloti* FtsZ overproducers decreased over 10-fold relative to the control within 4 h after IPTG induction, whereas cells containing the pWM176 vector did not decrease in viability (data not shown). This suggests that the branching cells were inhibited for cell division and could not recover.

To determine whether any structures could be seen inside the FtsZ1-overproducing cells that coincided with branch points, cell sections were examined by TEM (Fig. 5). The cell wall surrounding the branches and buds appeared to be intact. No obvious structural features were detectable with our methods that could be attributed to branching or budding, although we cannot rule out the possibility that such structures would be visible upon more exhaustive serial sectioning. Whereas most of the cells had midcell buds or branches, some had apparently normal midcell invaginations (Fig. 5A, arrow). The predominantly medial location of the branches suggests that the cell wall was breached near the cell midpoint to accommodate increased cell mass. We observed similar branches and lack of internal structural features with TEM of FtsZ2-overproducing cells (data not shown).

The branching and swelling phenotypes are not specific to *R. meliloti* FtsZ or to *R. meliloti* cells. To test whether the branching and swelling phenotypes in *R. meliloti* were due to specific effects of the *R. meliloti* FtsZ proteins, we overproduced *E. coli* FtsZ in the same expression system in *R. meliloti*. The branching phenotypes due to overproduction of *E. coli* FtsZ and *R. meliloti* FtsZ1 were indistinguishable; T-shaped cells were the majority in both cases (Fig. 6E and G). This result indicates that branching can be induced by expression of a heterologous *ftsZ* and is thus analogous to the filamentation caused by expression of *R. meliloti ftsZ1* in *E. coli*. This suggests that *E. coli* FtsZ can interfere with the *R. meliloti* cell division machinery, perhaps by polymerizing aberrantly or by forming unproductive copolymers with FtsZ1. It further suggests that the branching response is not dependent on overproduction of a branch-specific FtsZ but is in fact specific to the architectural constraints of the cell.

To demonstrate that the cell division inhibitory effects that we observed in *R. meliloti* could be observed in other species, we introduced the P_{tac}-*ftsZ1* plasmid into *A. tumefaciens* A136. The plasmid was unstable in this strain, perhaps because excess FtsZ1 was toxic. Even without IPTG induction, the cells were generally larger and more pleomorphic than cells without the plasmid (Fig. 6B), suggesting either that *ftsZ1* was expressed more efficiently in *A. tumefaciens* than in *R. meliloti* or that cell division in *A. tumefaciens* was more sensitive to the heterologous protein. Upon IPTG induction, cells further increased in mass and displayed multiple branches and invaginations, reminiscent of both FtsZ1 and FtsZ2 overproduction phenotypes in *R. meliloti* (Fig. 6C). These results suggest that *A. tumefaciens*, like *R. meliloti*, responds to cell division inhibition by branching and swelling instead of filamentation.

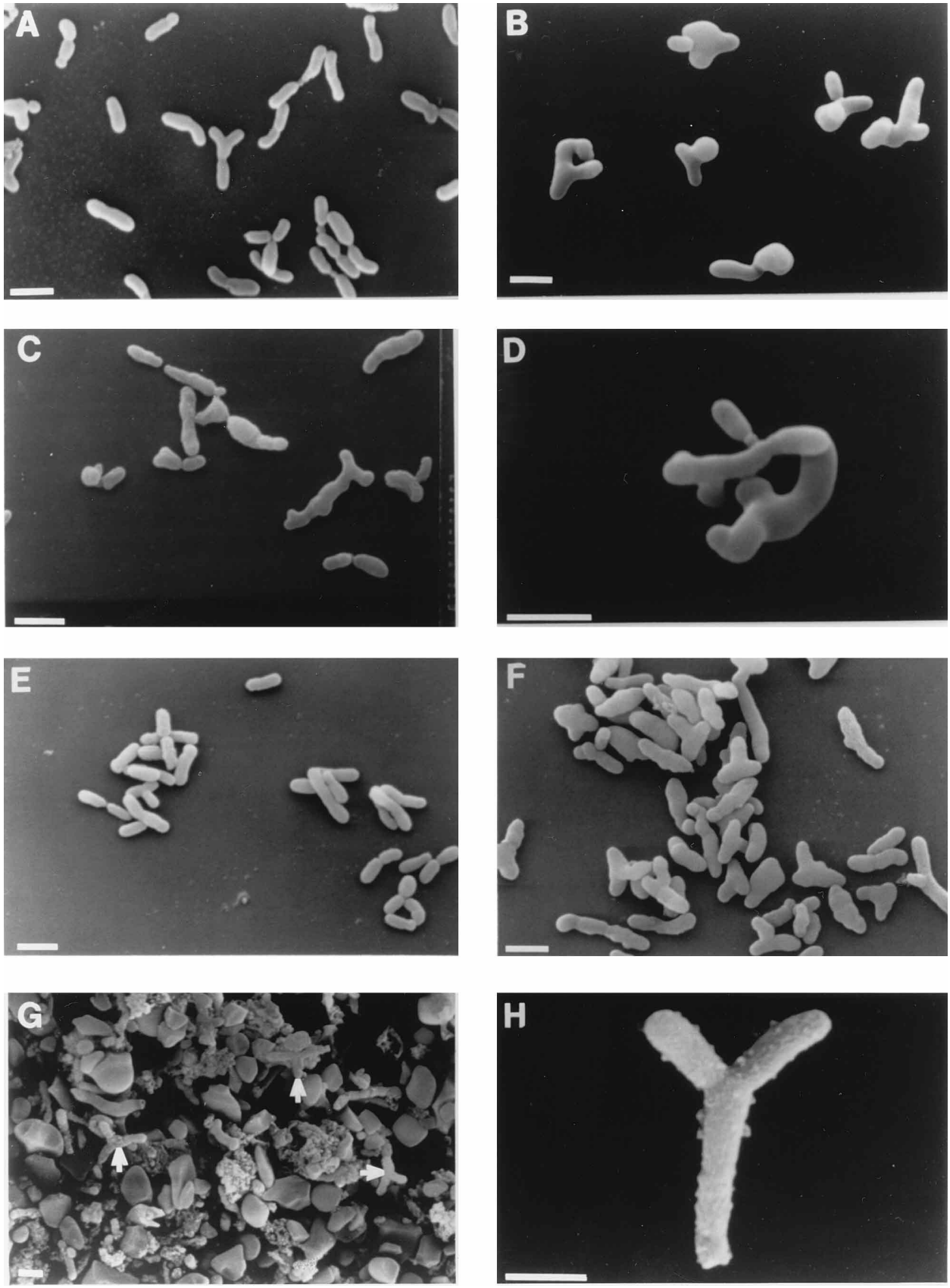

FIG. 4. Analysis of *R. meliloti* cells by SEM. (A to F) Effects of overproduction of FtsZ. WM249 cells with the following plasmids were grown to logarithmic phase in LB-tetracycline medium at 30°C and then either induced or not induced with 0.5 to 1 mM IPTG for 12 h. (A) pWM176 vector plus IPTG; (B) pWM186 (*ftsZ2*) plus IPTG; (C) pWM186 (*ftsZ2*); (D) pWM186 (*ftsZ2*) plus IPTG, showing a single branched cell; (E) pWM189 (*ftsZ1*); (F) pWM189 (*ftsZ1*) plus IPTG. (G and H) Morphology of *R. meliloti* bacteroids, shown for comparison. (G) Micrograph of a portion of a homogenized root nodule from alfalfa containing *R. meliloti*, showing bacteroids (arrows) and starch granules; (H) same as panel G, except an isolated bacteroid is shown. Bars = 2 μm.

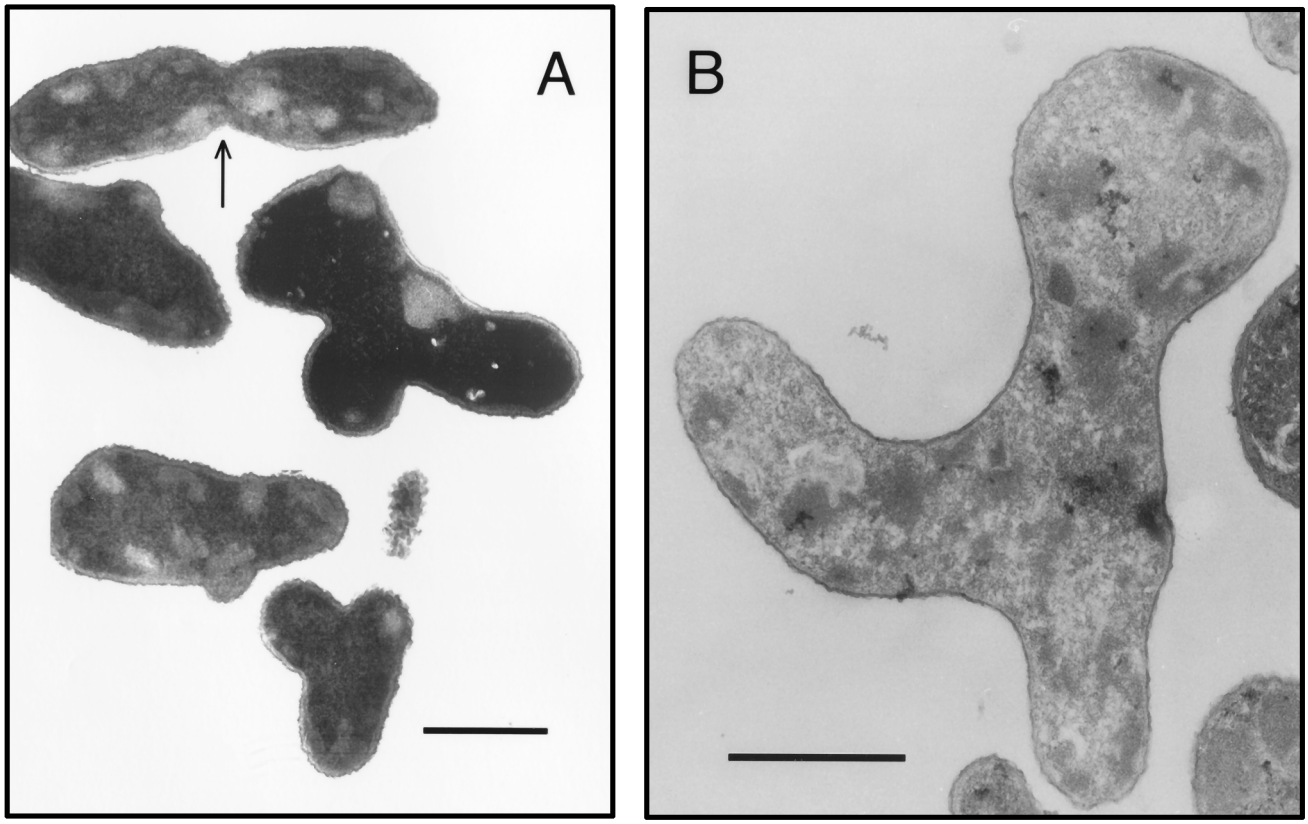

FIG. 5. TEM of *R. meliloti* overexpressing *ftsZ*. WM249/pWM189 (*ftsZ1*) cells were used. Cells were induced with 1 mM IPTG and processed for TEM as described in the text. (A) A composite of three separate photographs, showing cells at division (arrow) and at various stages of midcell branching. The arrow points to an apparently normal midcell invagination. (B) A single branching cell. Bars = 1 μm.

DISCUSSION

Normal cell division of *E. coli*, *B. subtilis*, and other rod-shaped bacteria occurs at the cell midpoint, resulting in two daughter cells, each with half the mass of the mother cell. Spherical bacteria, such as cocci and *rodA* mutants of *E. coli*, divide similarly. Blocking DNA replication, nucleoid segregation, or cell division in growing, rod-shaped *E. coli* or *B. subtilis* cells results in continued mass increase and growth using existing architectural parameters. For example, rods elongate into long filamentous cells and small spheres expand into large spheres. If cell division is resumed, daughter cells are generated that are morphologically indistinguishable from the mother filamentous cell. Similarly, resumption of several rounds of cell division in spherical cells yields spheres of unit size (9).

R. meliloti displays a dramatic alternative to this maintenance of cell shape. Instead of continuing growth only as a rod after a cell division block, the formation of new cytoplasm and wall appears to be partly targeted toward particular regions of the cell. The result is swelling, branching, or both, combined with limited elongation. Although *E. coli* can occasionally form branches under certain conditions, our data show that *R. meliloti* cells are clearly primed for branch formation. At first glance, the generation of swellings and branches appears to be a chaotic method of accommodating increased cell mass, in contrast to the ordered growth as filaments by *E. coli*. However, branched regions of *R. meliloti* cells, with the exception of those that have actually lysed (as with some cells treated with cephalexin or overproducing FtsZ2), are generally similar in shape and length to the mother cell from which the branch emerged. This observation, along with iterative branching seen in Fig. 4F, suggests that there is an orderly program for branching in *R. meliloti* and that cells opt to branch rather than to form a filament. In addition, branches seem to occur either at the cell poles to generate Y shapes or at midcell to generate T shapes. This placement is evidence that new growth may be targeted to particular regions of the cell. Our experiments with *A. tumefaciens* and the presence of Y-shaped cells in the conditional branching mutant (10) also suggest that similar targeting exists in that species.

Based on these results, we would not have expected to isolate *Rhizobium* or *Agrobacterium* cell division mutants by screening for filamentous cells under nonpermissive conditions, as was done in original filter enrichments for filamentous temperature-sensitive (*fts*) mutants of *E. coli* (29). In fact, a search for *fts* mutants of *R. meliloti* prior to this work was unsuccessful; our present results suggest that this type of mutant would not have been found even after an exhaustive search. Instead, obtaining temperature-sensitive cell division mutants may require a different type of enrichment, such as fluorescence-activated cell sorting of DAPI-stained cells or enrichment for multinucleate, branched cells under nonpermissive conditions.

What is the mechanism of branch creation? Our EM data and data from *Agrobacterium* microculture studies (11) suggest that branches begin as a breach of the determinants of rod shape in the cell wall. This breach can occur at or near the division site in the T-shaped cells resulting from FtsZ overpro-

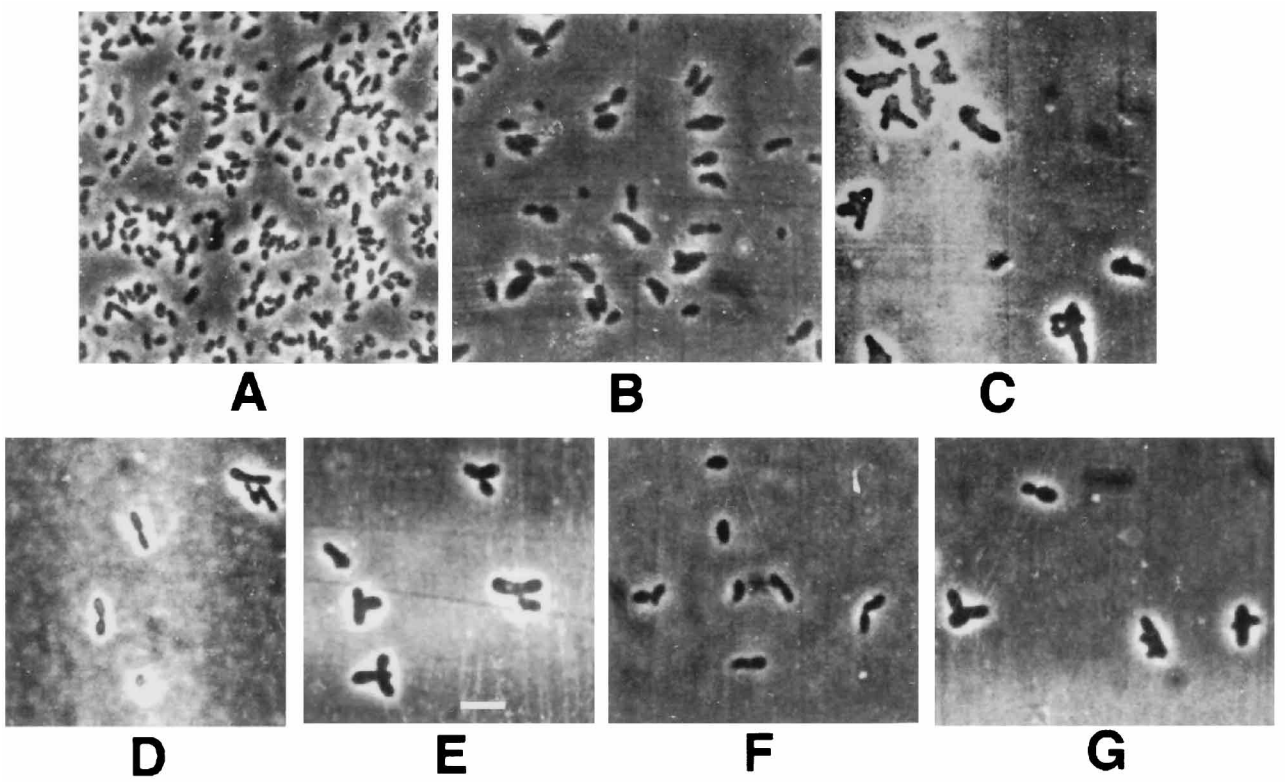

FIG. 6. Branching is not specific to *R. meliloti* FtsZ and can be induced in *A. tumefaciens* cells. Phase-contrast images were taken of cells grown to mid-logarithmic phase, then induced or not induced with 1 mM IPTG, and then grown for 12 h. The *A. tumefaciens* strains containing plasmids were unstable in the presence of tetracycline and needed to be grown freshly from frozen stocks. (A) *A. tumefaciens* A136; (B) A136/pWM189 (*ftsZ1*); (C) A136/pWM189 plus IPTG; (D) *R. meliloti* Rm1021/pMK3 (*E. coli ftsZ* opposite P_{tac}) plus IPTG; (E) Rm1021/pMK4 (*E. coli ftsZ* driven by P_{tac}) plus IPTG; (F) Rm1021/pMK4; (G) Rm1021/pWM189 plus IPTG. Bar = 4 μm.

duction or at the pole in the case of Y-shaped cells induced by mitomycin C or nalidixic acid. It is important to emphasize that this breach is often controlled, since the emerging branch is stable and surrounded by a wall.

One model for the initiation of branching involves FtsZ. FtsZ has a key cytoskeletal role in redirecting the cell wall from the elongation to the invagination mode and thus initiates new points and directions of growth. Perhaps FtsZ in *R. meliloti* has an additional role in nucleating growth at new cellular sites. A priori, FtsZ2 would be a likely candidate for such a role, except that we have shown that an *ftsZ2* deletion mutant is proficient at branching (16). Instead, FtsZ1, with its unique large C-terminal extension, could be involved in this process, either directly or via interactions with another protein that is specific to *R. meliloti*. One mechanism by which *E. coli* FtsZ could cause the same phenotype is through coassembly with *R. meliloti* FtsZ1, thereby altering its normal function. This scenario is somewhat analogous to the ability of excess *R. meliloti* FtsZ to block *E. coli* cell division, except that the *Rhizobium* model would predict that *E. coli* FtsZ actually stimulates the ability of FtsZ1 to form branches. A similar model could explain the induction of branching in *A. tumefaciens* by *E. coli* FtsZ. The idea of FtsZ nucleating new sites for growth has also been hypothesized for *Caulobacter crescentus*, in which stalk biosynthesis may involve FtsZ (5). Interestingly, *C. crescentus* also has an FtsZ protein with an extended C terminus similar to that of *R. meliloti* FtsZ1 (23).

An alternative model is that branching is not due to direct action of FtsZ but instead is a general response to cell cycle inhibition. For example, *Rhizobium* cell shape constraints may simply be more relaxed than those of *E. coli*. In support of this idea is the extreme pleomorphism of *Rhizobium* cells under certain nutritional conditions (15, 28). In addition, the branching caused by mitomycin C may be induced via a pathway independent of FtsZ. However, the facts that dividing *R. meliloti* cells maintain their rod shape and that they seem to regulate branch production when not dividing suggest that there are constraints in place. One way to determine whether FtsZ has a direct effect on branching might be to assay for branching after depletion of FtsZ1 in the cell.

Morphological characteristics of *R. meliloti* cells were correlated with the particular treatments used to inhibit cell division. Cells treated with the DNA replication inhibitors nalidixic acid and mitomycin C elongated and, especially with mitomycin C, often branched at one pole to become Y shaped. It is likely that nalidixic acid did not allow as much branching because, unlike mitomycin C, it significantly inhibited growth. Interestingly, multiple branches were uncommon with the DNA replication inhibitors. On the other hand, cells overproducing FtsZ were usually swollen and more often T shaped, and they often exhibited multiple branches. The preponderance of multiply branched cells during FtsZ overproduction can be explained by the continuation of DNA replication, forcing the cells to achieve a higher cell mass than when DNA replication is inhibited and therefore requiring new cell surface synthesis. We speculate that Y-shaped cells arise from a breach of the cell wall at a growing pole whereas T-shaped cells result from a similar breach at the cell division site; the latter effect

may be due to the action of FtsZ1. The FtsZ-induced branching is probably not due to a general stress response to protein overproduction. First, it would be predicted that such a response should generate mainly Y-shaped cells, not the T-shaped and other forms observed here, since Y-shaped cells are produced by DNA-damaging treatments. Second, GFP overproduction had no effect on cell shape, making such a nonspecific cause less likely.

There is a striking similarity between the shape of the mitomycin C-induced Y-shaped *R. meliloti* cells and that of mature endosymbiotic bacteroids (Fig. 4G and H). Mature bacteroids contain less DNA than logarithmic-phase free-living cells but more DNA than those in stationary phase (33). It has been hypothesized that these bacteroids undergo a single final round of DNA replication and then arrest their cell cycle, all while their cell mass is still increasing (4). In addition, it is reasonable to assume that our logarithmically growing cells treated with mitomycin C contained less DNA than similarly grown cells not exposed to the drug. Therefore, the amount of DNA in these drug-treated cells may be similar to that of bacteroids. We propose that the polar swellings and Y shapes of bacteroids are caused by blockage of their DNA replication-segregation cycle when they are inside the plant cell, which we have mimicked by inhibiting DNA dynamics in free-living cells with drugs. The unusual shapes of bacteroids of other *Rhizobium* species could also be explained by this model.

It is not clear how widespread the branching response to cell cycle perturbations is or what advantages branching might confer on the cell. Other members of the alpha proteobacterial group, such as *Caulobacter* and *Rhodobacter* species, form filaments and do not tend to branch (12, 34), although *Caulobacter* stalks can branch (23). However, differences in spatial distribution of cell mass increase may be common in this group. For example, *Hyphomicrobium neptunium* normally reproduces by budding, but inhibition of DNA synthesis by nalidixic acid blocks budding and instead induces significant stalk elongation (32). One reason to branch is to increase the area of the cell for foraging; *Streptomyces* species carry this strategy to an extreme. However, branching, unlike filamentation, also would seem to destroy the architectural integrity of the unit cell, making it unlikely that the cell could recover from branching to divide again. Further work on determining the factors that are responsible for branching should provide answers to some of these key questions about microbial morphology and survival.

ACKNOWLEDGMENTS

We thank Sharon Long and members of her laboratory for support during the initial phase of this work and for many helpful discussions. We are grateful to Melanie Barnett for providing us with strain MB501, Dan Gage for the GFP overproducer, Fran Thomas for assistance with EM techniques, and Tom Vida for the use of his microscope facility.

This work was supported in part by grants from the NSF (MCB-9410840) and the USDA (94-37305-0958) to W.M.

REFERENCES

1. **Ackerlund, T., K. Nordstrom, and R. Bernander.** 1993. Branched *Escherichia coli* cells. Mol. Microbiol. **10:**849–858.
2. **Addinall, S. G., E. Bi, and J. Lutkenhaus.** 1996. FtsZ ring formation in *fts* mutants. J. Bacteriol. **178:**3877–3884.
3. **Begg, K. J., and W. D. Donachie.** 1985. Cell shape and division in *Escherichia coli*: experiments with shape and division mutants. J. Bacteriol. **163:**615–622.
4. **Bisseling, T., R. C. van den Bos, A. van Kammen, M. van der Ploeg, P. van Duijn, and A. Houwers.** 1977. Cytofluorometrical determination of the DNA contents of bacteroids and corresponding broth-cultured *Rhizobium* bacteria. J. Gen. Microbiol. **101:**79–84.
5. **Brun, Y. V., G. Marczynski, and L. Shapiro.** 1994. The expression of asymmetry during *Caulobacter* cell differentiation. Annu. Rev. Biochem. **63:**419–450.
6. **Buxton, P., and I. B. Holland.** 1983. Two pathways of division inhibition in UV-irradiated *E. coli*. Mol. Gen. Genet. **190:**309–314.
7. **Degnen, S. T., and A. Newton.** 1972. Dependence of cell division on the completion of chromosome replication in *Caulobacter crescentus*. J. Bacteriol. **110:**852–856.
8. **Donachie, W. D.** 1993. The cell cycle of *Escherichia coli*. Annu. Rev. Microbiol. **47:**199–230.
9. **Donachie, W. D., S. Addinall, and K. Begg.** 1995. Cell shape in chromosome partition in prokaryotes, or why *E. coli* is rod-shaped and haploid. Bioessays **17:**569–576.
10. **Fujiwara, T., and S. Fukui.** 1972. Isolation of morphological mutants of *Agrobacterium tumefaciens*. J. Bacteriol. **110:**743–746.
11. **Fujiwara, T., and S. Fukui.** 1974. Unidirectional growth and branch formation of a morphological mutant, *Agrobacterium tumefaciens*. J. Bacteriol. **120:**583–589.
12. **Genthner, F. J., and J. D. Wall.** 1984. Isolation of a recombination-deficient mutant of *Rhodopseudomonas capsulata*. J. Bacteriol. **160:**971–975.
13. **Guzman, L.-M., J. J. Barondess, and J. Beckwith.** 1992. FtsL, an essential cytoplasmic membrane protein involved in cell division in *Escherichia coli*. J. Bacteriol. **174:**7716–7728.
14. **Helmstetter, C. E., and O. Pierucci.** 1968. Cell division during inhibition of deoxyribonucleic acid synthesis in *Escherichia coli*. J. Bacteriol. **95:**1627–1633.
15. **Kaneshiro, T., F. L. Baker, and D. E. Johnson.** 1983. Pleomorphism and acetylene-reducing activity of free-living rhizobia. J. Bacteriol. **153:**1045–1050.
16. **Latch, J. N., and W. Margolin.** Unpublished results.
17. **Long, S. R., and B. J. Staskawicz.** 1993. Prokaryotic plant parasites. Cell **73:**921–935.
18. **Ma, X., D. W. Ehrhardt, and W. Margolin.** 1996. Colocalization of cell division proteins FtsZ and FtsA to cytoskeletal structures in living *Escherichia coli* cells by using green fluorescent protein. Proc. Natl. Acad. Sci. USA **93:**12998–13003.
19. **Margolin, W., J. C. Corbo, and S. R. Long.** 1991. Cloning and characterization of a *Rhizobium meliloti* homolog of the *Escherichia coli* cell division gene *ftsZ*. J. Bacteriol. **173:**5822–5830.
20. **Margolin, W., and S. R. Long.** 1994. *Rhizobium meliloti* contains a novel second homolog of the cell division gene *ftsZ*. J. Bacteriol. **176:**2033–2043.
21. **Meade, H. M., S. R. Long, G. B. Ruvkun, S. E. Brown, and F. M. Ausubel.** 1982. Physical and genetic characterization of symbiotic and auxotrophic mutants of *Rhizobium meliloti* induced by transposon Tn*5* mutagenesis. J. Bacteriol. **149:**114–122.
22. **Ogawa, J., and S. R. Long.** 1995. The *Rhizobium meliloti groELc* locus is required for regulation of early nod genes by the transcription activator NodD. Genes Dev. **9:**714–729.
23. **Quardokus, E., N. Din, and Y. V. Brun.** 1996. Cell cycle regulation and cell type-specific localization of the FtsZ division initiation protein in *Caulobacter*. Proc. Natl. Acad. Sci. USA **93:**6314–6319.
24. **Rinken, R., and W. Wackernager.** 1992. Inhibition of the *recBCD*-dependent activation of Chi recombinational hot spots in SOS-induced cells of *Escherichia coli*. J. Bacteriol. **174:**1172–1178.
25. **Sobral, B. W. S., R. J. Honeycutt, A. G. Atherly, and M. McClelland.** 1991. Electrophoretic separation of the three *Rhizobium meliloti* replicons. J. Bacteriol. **173:**5173–5180.
26. **Spratt, B. G.** 1975. Distinct penicillin binding proteins involved in the division, elongation, and shape of *Escherichia coli* K12. Proc. Natl. Acad. Sci. USA **72:**2999–3003.
27. **Spurr, A. R.** 1969. A low-viscosity epoxy resin embedding medium for electron microscopy. Ultrastruct. Res. **26:**41–43.
28. **Urban, J. E., and F. B. Dazzo.** 1982. Succinate-induced morphology of *Rhizobium trifolii* 0403 resembles that of bacteroids in clover nodules. Appl. Environ. Microbiol. **44:**219–226.
29. **van de Putte, P., J. van Dillewin, and A. Rorsch.** 1964. The selection of mutants of *Escherichia coli* with impaired cell division at elevated temperatures. Mutat. Res. **1:**121–128.
30. **Ward, J. E., and J. Lutkenhaus.** 1985. Overproduction of FtsZ induces minicells in *E. coli*. Cell **42:**941–949.
31. **Watson, B., T. C. Currier, M. P. Gordon, M.-D. Chilton, and E. W. Nester.** 1975. Plasmid required for virulence of *Agrobacterium tumefaciens*. J. Bacteriol. **123:**255–264.
32. **Weiner, R. M., and M. A. Blackman.** 1973. Inhibition of deoxyribonucleic acid synthesis and bud formation by nalidixic acid in *Hyphomicrobium neptunium*. J. Bacteriol. **116:**1398–1404.
33. **Wheatcroft, R., D. G. McRae, and R. W. Miller.** 1990. Changes in the *Rhizobium meliloti* genome and the ability to detect supercoiled plasmids during bacteroid development. Mol. Plant-Microbe Interact. **3:**9–17.
34. **Winzeler, E., and L. Shapiro.** 1995. Use of flow cytometry to identify a *Caulobacter* 4.5 S RNA temperature-sensitive mutant defective in the cell cycle. J. Mol. Biol. **251:**346–365.